TU Delft

Delft University of Technology

Document Version
Final published version

Licence
Dutch Copyright Act (Article 25fa)

Citation (APA)
Sirotti, M., Staquet, S., Delsaute, B., Li, Z., Ye, G., & Cizer, Ö. (2026). Restrained Shrinkage of Alkali-Activated Materials. In G. Ye, & F. Dehn (Eds.), *Mechanical Properties of Alkali-Activated Materials: State-of-the-Art Report of the RILEM Technical Committee 294-MPA* (pp. 503-523). (RILEM State-of-the-Art Reports; Vol. 46). Springer. https://doi.org/10.1007/978-3-032-07116-3_13

Important note
To cite this publication, please use the final published version (if applicable).
Please check the document version above.

Copyright
In case the licence states “Dutch Copyright Act (Article 25fa)”, this publication was made available Green Open Access via the TU Delft Institutional Repository pursuant to Dutch Copyright Act (Article 25fa, the Taverne amendment). This provision does not affect copyright ownership.
Unless copyright is transferred by contract or statute, it remains with the copyright holder.

Sharing and reuse
Other than for strictly personal use, it is not permitted to download, forward or distribute the text or part of it, without the consent of the author(s) and/or copyright holder(s), unless the work is under an open content license such as Creative Commons.

Takedown policy
Please contact us and provide details if you believe this document breaches copyrights.
We will remove access to the work immediately and investigate your claim.

This work is downloaded from Delft University of Technology.

Restrained Shrinkage of Alkali-Activated Materials

Marco Sirotti, Stéphanie Staquet, Brice Delsaute, Zhenming Li, Guang Ye, and Özlem Cizer

Abstract The formation of micro-cracks due to restrained shrinkage is a significant concern for the durability and in-service implementation of alkali-activated materials (AAM). These cracks develop as a result of partial or total restrained deformations which occur when the material's properties are still evolving, and the deformation rate is high. This makes AAM especially susceptible to cracking during this critical early stage, leading to potential long-term durability issues. Therefore, it is particularly crucial to understand their restrained shrinkage behavior and early-age cracking risk. This chapter discusses two approaches for assessing the cracking sensitivity of AAM with a particular focus on the empirical method. It reviews the existing testing devices for evaluating restrained shrinkage and cracking in AAM, and compares and discusses key findings from the literature.

Keywords Ring test · Cracking · Alkali-activated materials · Restrained strain · Stress

M. Sirotti · S. Staquet (✉) · B. Delsaute
BATir Department, Université Libre de Bruxelles ULB, Brussels, Belgium
e-mail: stephanie.staquet@ulb.be

B. Delsaute
CRIC-OCCN, Brussels, Belgium

Z. Li
School of Civil and Environmental Engineering, Harbin Institute of Technology, Shenzhen, China

Guangdong Provincial Key Laboratory of Intelligent and Resilient Structures for Civil Engineering, Harbin Institute of Technology, Shenzhen, China

G. Ye
Section Materials and Environment, Department of 3Md, Faculty of Civil Engineering and Geosciences, Delft University of Technology, Delft, The Netherlands

Ö. Cizer (✉)
Department of Civil Engineering, Materials and Constructions, KU Leuven, Leuven, Belgium
e-mail: ozlem.cizer@kuleuven.be

© RILEM 2026

G. Ye and F. Dehn (eds.), *Mechanical Properties of Alkali-Activated Materials*, RILEM State-of-the-Art Reports 46, https://doi.org/10.1007/978-3-032-07116-3_13

1 Introduction

Similar to Portland cement paste [1], alkali-activated materials (AAM) are complex systems that undergo continuous changes as they transition from a liquid to a solid state. During this phase, the material sets and its mechanical properties start to develop. As discussed in Chaps. "Autogenous Shrinkage of Alkali-Activated Materials" (autogenous deformation) and "Creep Properties of Alkali-Activated Concretes" (drying shrinkage), during this early stage the shrinkage of AAM induced by the chemical reaction (autogenous shrinkage) and desiccation (drying shrinkage) can be very significant, which is often far exceeding that of traditional Portland cement concrete. Autogenous shrinkage for Portland cement (PC) paste can reach up to 1100 μm/m when its water/cement ratio is between 0.3 and 0.4 [2], while for AAM, it remains between 3000 and 8000 μm/m depending on several parameters such as alkali dosage and silicate modulus [3]. Ballekere Kumarappa et al. [4] and Uppalapati [5] have demonstrated that although the autogenous strain of AAM is reduced at mortar scale (between 1500 and 5000 μm/m) due to the restraint induced by the sand and the low E-modulus at early age when the autogenous strain develops, it remains substantially higher than that of Portland cement mix (about 500 μm/m). Additionally, the drying shrinkage of AA blast-furnace slag concrete has been reported to be up to three times higher than that of PC concrete under the same temperature (23 °C) and relative humidity (50%) conditions [6]. These shrinkages, autogenous and drying ones, result in important volume changes, which can lead to the buildup of tensile stresses when the deformation is restrained. In practice, such restraints in concrete material are unavoidable and can arise from either internal factors (e.g. steel reinforcement and aggregates) or external ones (e.g. adjacent structures). Consequently, the volume change of concrete is somewhat limited, leading to the development of internal tensile stresses from shrinkage deformations. If these tensile stresses from restrained shrinkage surpass the material's tensile strength, cracking occurs, which can pose a significant threat to the material's and structure's durability throughout its service life (Fig. 1). Given that AAM show greater shrinkage deformation and a higher risk of early-age cracking compared to cement-based materials (CBM), it is essential to evaluate and control this cracking behavior for safe and reliable applications of these materials.

The early-age cracking sensitivity of AAM refers to the material's tendency to develop cracks during its early-age stages of setting and hardening. This is primarily driven by the material's shrinkage behavior, tensile strength development, and the conditions under which it cures. To study the cracking sensitivity, two approaches are used: analytical approach and empirical approach.

Analytical approach: According to the superposition principle which is commonly used to make the mathematical decoupling between the various sources of the strains, the total strain is the sum of the autogenous strain ε_{au}, the thermal strain ε_{th}, the drying strain ε_{ds}, the elastic strain ε_{el} and the creep strain ε_{cr} as indicated in Eq. 1. Stresses are defined according to Eq. 2, where σ is the stress, t is the age of the concrete, t′ is the age of the concrete at loading, $J(t, t')$ is the compliance function, $E(t')$ is the

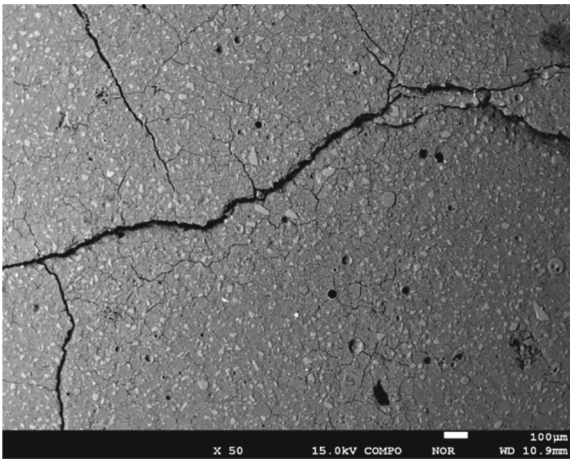


Fig. 1 Micro-cracking of the sodium silicate activated slag at 7 days

elastic modulus and $C(t, t')$ is the specific creep. Then, stress can be computed based on the development of each property since the material's setting.

$$\varepsilon_{tot} = \varepsilon_{au} + \varepsilon_{th} + \varepsilon_{ds} + \varepsilon_{el} + \varepsilon_{cr} \tag{1}$$

$$\varepsilon_{el}(t') + \varepsilon_{cr}(t, t') = \sigma \cdot \mathrm{J}(\mathrm{t}, \mathrm{t}') = \sigma \cdot \left(\frac{1}{\mathrm{E}(\mathrm{t}')} + C(t, t') \right) \tag{2}$$

Empirical approach: Over the last decades, passive and active restrained shrinkage methods have been developed to investigate the cracking sensitivity of cement-based materials. In passive restrained shrinkage tests, the specimen is restrained from the time of casting by a frame and the degree of restrain is determined by the difference of stiffness between the sample and the testing device. Even though several passive methods exist, the most commonly used method is the ring test [7–9]. Active restrained shrinkage tests allow for continuous control of the restraint throughout the test. Temperature Stress Testing Machine (TSTM) is primarily used to actively study the restrained shrinkage [10, 11].

Although both approaches are feasible, the "passive" empirical approach is generally preferred for studying the cracking sensitivity of cement-based materials. This preference is due to (i) the simplicity and lower cost of ring tests compared to the TSTM and (ii) the challenges involved in accurately defining free deformation and viscoelastic properties from the time of setting. Nevertheless, recent progress has enabled the evolution of autogenous and thermal deformations as well as the evolution of the modulus of elasticity and the specific creep function from the setting time using a very limited number of tests [12, 13]. In this chapter, only results related to empirical approaches are presented.

In this chapter, a brief overview of the testing devices used to study the restrained shrinkage is presented. Following this, the key findings from the literature are compared and discussed.

2 Testing Devices

2.1 Ring Test

Tests on restrained shrinkage are typically used to assess the cracking sensitivity of cementitious materials at an early age under restrained conditions, simulating real-world scenarios. For this purpose, various methodologies have been developed in which the shrinkage of the testing specimen is mechanically restrained, leading to the development of tensile stresses and eventual cracking [1].

ASTM C1581 [9] recommended a ring test with specific dimensions to estimate the early-age cracking tendency of cement-based materials under restraint shrinkage conditions. This method is the most common test method used for the quantification of the material's performance by estimating the age at which cracking occurs, the number of cracks formed and the average and maximum width of the cracks [1]. According to ASTM C1581 and also AASHTO PP34-99 standard, the ring test consists of two concentric rings: an inner steel ring and an outer concrete ring (Fig. 2). The shrinkage of the concrete ring is restrained by the steel ring, creating stresses in the concrete and exerting surface pressure on the steel. Four strain gauges, attached to the inner surface of the steel ring, measure the resulting deformations. A sudden drop in the steel ring's deformation indicates the formation of cracking in the concrete. The age at which this cracking occurs depends on the dimensions of the restrained ring and the tensile stress distribution across the concrete's cross-section. Several experimental testing devices exist, which differ based on key parameters such as:

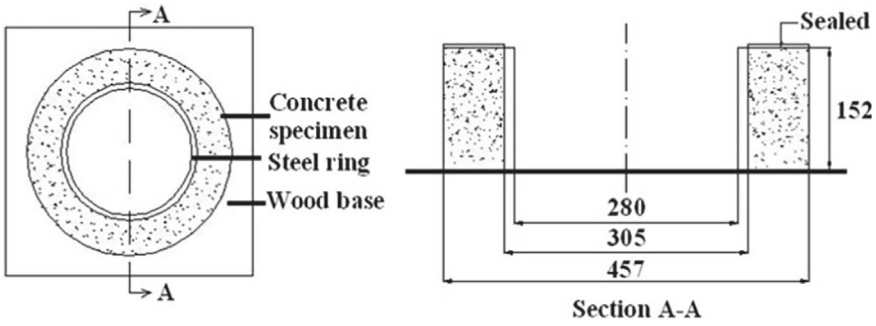


Fig. 2 Ring test according to AASHTO standard with dimensions in mm [14]

Table 1 Geometry of the ring test used by different studies

Author(s)	Diameter inner ring (mm)	Diameter outer ring (mm)	Height (mm)
Sirotti et al. [15], AASHTO standard	305	381	150
Li et al. [16]	115	250	75
Blomart [17], AASHTO standard	305	381	150
Ling et al. [18]	100	150	30
Aboshia et al. [19], ASTM standar	330	410	150

- Dimensions of the restraining ring: inner and outer diameters, and height of the core material
- Material of the restraining ring: commonly steel or invar
- Scale of the tested material: paste, mortar or concrete
- Degree of restraint: which influences the level of shrinkage restriction applied to the sample.

All these parameters influence the evolution of the strain and stress in the tested material in terms of magnitude and kinetics. The curing condition of the samples, such as type of curing, curing time and curing temperature, can also influence the material behavior. All these aspects are discussed in detail in [7, 8]. Many researchers have been quantifying the potential of shrinkage cracking in cementitious materials by using a ring test with different dimensions, other than ASTM standard ring as indicated in Table 1.

2.2 Temperature Stress Testing Machine (TSTM)

The detailed development of an TSTM device is described in detail by Delsaute and Staquet [1]. It consists of a horizontal dog-bone-shaped sample in which one end is fixed while the displacement or the force applied to the other one is controlled in order to partially or fully restrain the shrinkage of the specimen. A scheme of a TSTM device is shown in Fig. 3. The only difference between the devices used in the different studies is the width of the prismatic section which ranges from 100 to 150 mm, while the length and height are constant at 1000 mm and 100 mm, respectively.

When the shrinkage or swelling of the sample in the moving part reaches a certain threshold of a few microstrains, a load or displacement is applied to bring the sample to its initial position. During the next cycle, the load or displacement is maintained at a constant level until the deformation once again reaches the threshold and the load is increased or reduced. This cycle continues until the sample ultimately cracks. A scheme of the protocol is shown in Fig. 4.

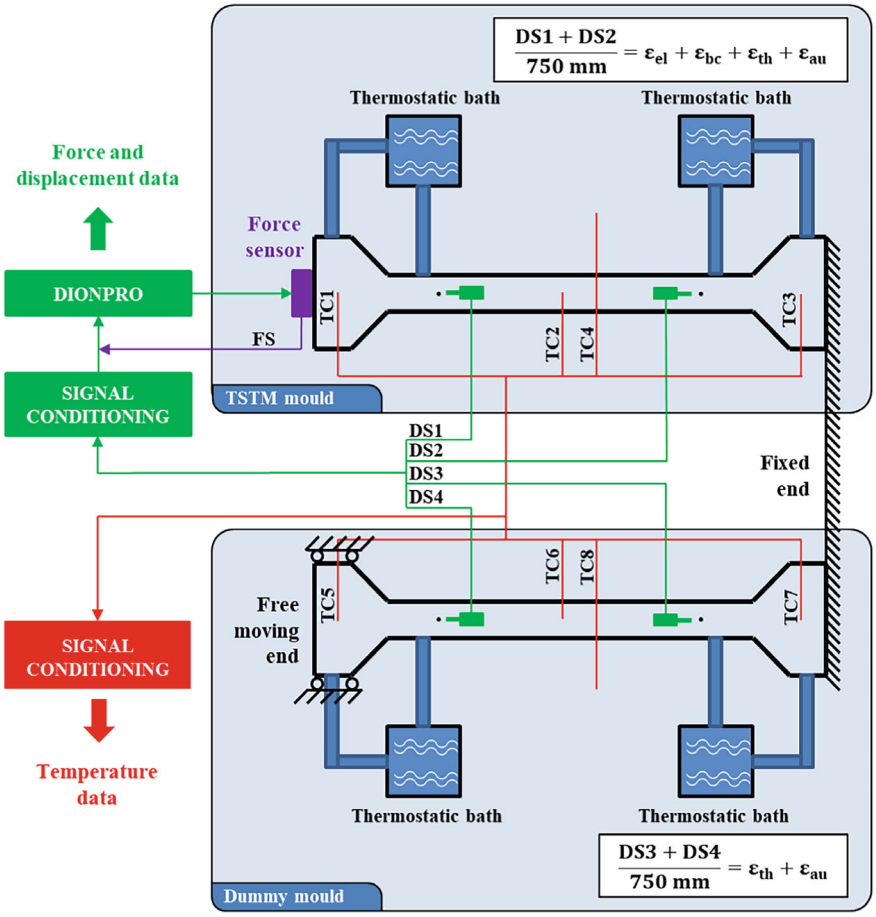


Fig. 3 Scheme of the TSTM device and testing protocol [1]

3 Results from the Literature

The cracking sensitivity of AAM at early age is directly related to the free deformation and the development of the mechanical properties, which are influenced by the composition of the material. In the case of AAM, it is important to distinguish between precursor and alkaline activator. The former represents the solid component that provides the structure-forming oxides, while the latter is the liquid solution (unless one-part mixing is applied [20]) that dissolves the solid oxides and initiates the reaction. Commonly investigated precursors include ground-granulated blast furnace slag (GGBFS or slag), fly ash (FA), and metakaolin (MK), while the most frequently used activators are sodium silicate (SS) and sodium hydroxide (SH). While numerous other materials can react to form AAM, they are typically less studied and

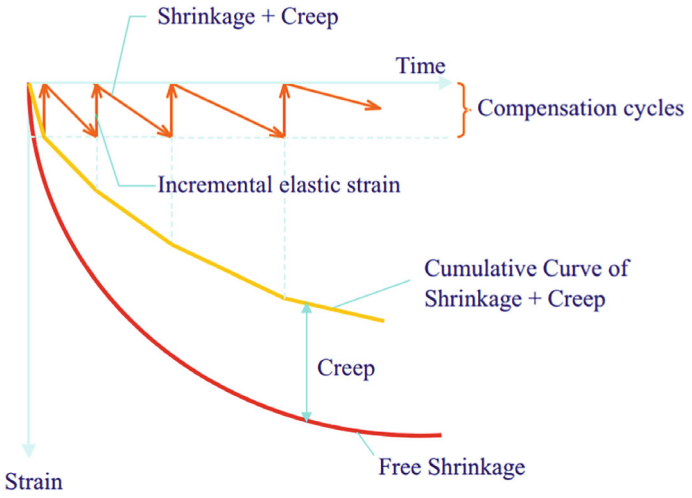


Fig. 4 Protocol of the TSTM device based on the calculation of creep strain from the measurements of restrained and free shrinkage in companion specimens [11]

widespread, so they will not be included in this analysis. Often, different precursors and/or activators are combined in order to improve the properties of the final product [21].

3.1 Restrained Shrinkage in Autogenous Conditions

Sirotti et al. [15] investigated the cracking sensitivity of AAMs made from four different slag compositions. The molar concentration of the NaOH activator used in this study was 2 mol/L (2M) or 8 mol/L (8M) with a solution-to-binder mass ratio (s/b) of 0.5 or 0.8; the binder was blast-furnace slag. All compositions were tested at the mortar scale with a sand-to-paste ratio of 1 due to workability issues in high molarity conditions. The cracking sensitivity was studied using the ring test. Figure 5 shows the strain over time for the different compositions, indicating that changes in the s/b ratio significantly influence the behavior of alkali-activated slag. Specifically, when the s/b ratio increases to 0.8, none of the compositions exhibited cracking within the first 600 h. In addition, the effect of increasing the molarity of the activating solution depends on the s/b: at an s/b ratio of 0.5, higher molarity leads to increased maximum strain, whereas at s/b = 0.8, the maximum strain decreases with rising molarity. For compositions with low s/b ratios, an increase in molarity also delays the onset of cracking. The authors further upscaled the autogenous shrinkage data from Lacante et al. [22] to the mortar scale using the model from Delsaute [12], where the two boundary conditions provide the lower and upper extremes in Fig. 6. The results show that increasing the s/b ratio reduces shrinkage, while higher molarity results in

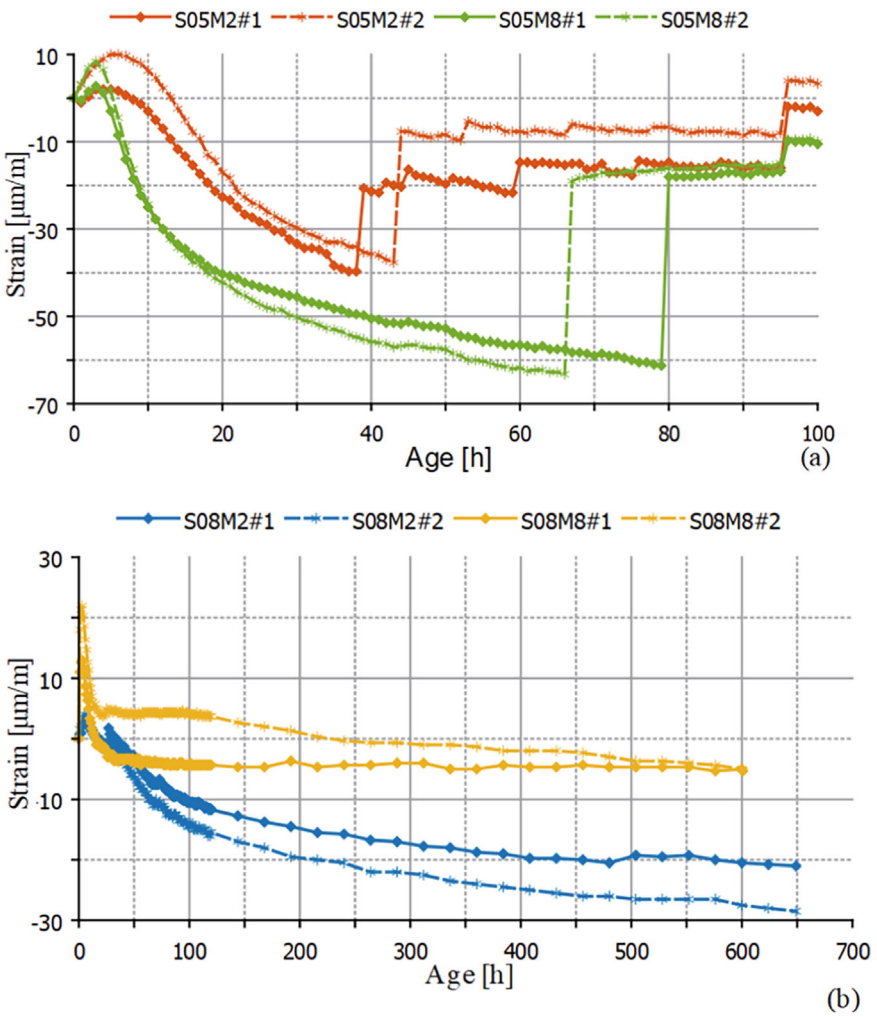


Fig. 5 Ring test comparison in sealed conditions for 0.5 (**a**) and 0.8 s/b (**b**) [15] (the term of the mixtures is formed by their s/b, i.e. 0.5 or 0.8, and molarity of the activator, i.e. 2 or 8 mol/L)

increased shrinkage. Although there is good agreement between free and restrained shrinkage at an s/b ratio of 0.5, the ring test reveals lower strain for paste or mortar with s/b = 0.8 and 8 M, likely due to significant swelling at the beginning of the test.

In another study, Li et al. [16] compared the cracking sensitivity of two different compositions: slag and a binary system composed of 50% slag and 50% fly ash. The alkaline activator was a mixture of sodium silicate and sodium hydroxide. The tests were carried out at the concrete scale using a TSTM device. The results presented in Fig. 7 show that the slag-only composition (AAS) exhibits a later cracking age and a higher maximum stress than the composition containing fly ash (AASF). In addition,

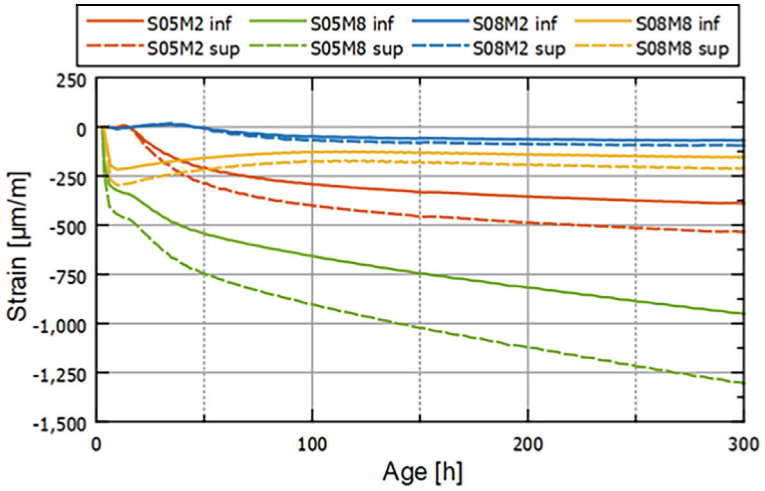


Fig. 6 Upscaled autogenous shrinkage using two different boundary conditions [15] (the term of the mixtures is formed by their s/b, i.e. 0.5 or 0.8, and molarity of the activator, i.e. 2 or 8 mol/L)

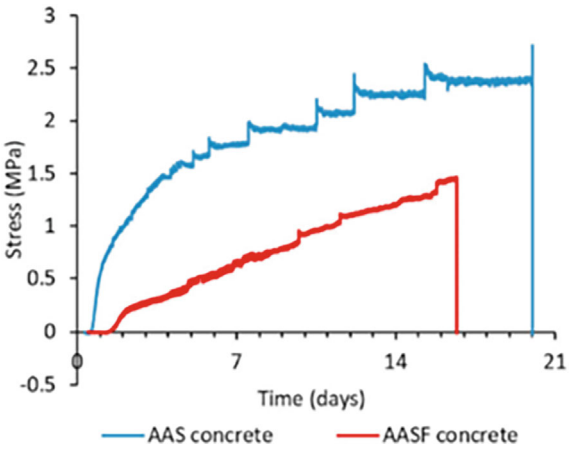


Fig. 7 Autogenous shrinkage-induced stress in AAS (slag based) and in AASF (slag and fly ash based) concretes obtained by TSTM measurements [16]

the stress rate development of the slag-only composition is initially very rapid but slows down considerably at later ages, while AASF presents an almost constant rate of stress development over time. When comparing these results with the autogenous shrinkage in Fig. 8, it becomes evident that substituting fly ash nearly halves the magnitude of autogenous shrinkage at 21 days. The higher shrinkage observed in the slag composition, despite its later cracking, is attributed to the introduction of fly ash, which reduces tensile strength. Consequently, the maximum stress in the material may occur before failure under tension [16].

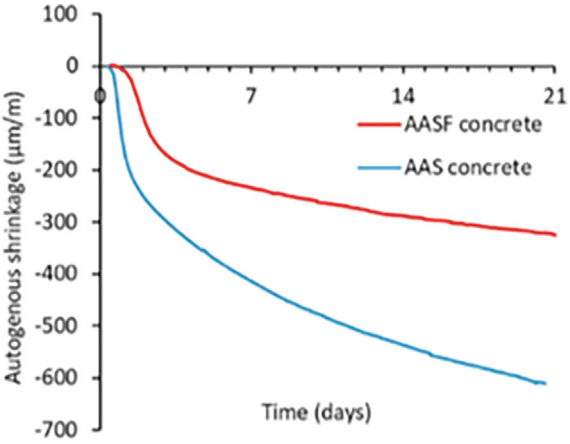


Fig. 8 Autogenous shrinkage of AAS (slag based) and in AASF (slag and fly ash based) concretes obtained from Autogenous deformation testing machine measurements [16]

Another study compared the same slag and slag-fly ash compositions with different Portland cement compositions [23]. Specifically, the authors studied three different concretes obtained from the mix of clinker and blast furnace slag in different proportions: CEM I 52.5 N, CEM III/A 42.5 LA, and CEM III/B 42.5 HSR LA, in which the respective amount of slag is 0, 42.5, and 75%. The water and aggregate contents of cement and alkali-activated concretes were kept the same. Once again, the tests were carried out using the TSTM. The results shown in Fig. 9 show that the maximum stress in restrained conditions is comparable to the one of AAS in all cases, while the cracking he cracking times differ significantly, with all cement-based compositions cracking much earlier than the alkali-activated ones. On the other hand, the free shrinkage test shown in Fig. 10 presents different results: all three compositions exhibit significantly lower shrinkage compared to the alkali-activated concretes, suggesting that shrinkage alone is not the only driver of cracking. The authors also tested the splitting tensile strength (Fig. 11). They concluded that the earlier cracking age is attributed to the faster rate of stress evolution in cement concretes compared to alkali-activated ones. The relaxation phenomenon in slag and fly ash-based compositions plays a crucial role in delaying concrete cracking [23]. An interesting result provided by the authors concerns the degree of reaction (DoR) of the materials. They plotted the stress evolution in the TSTM against the degree of reaction obtained from the heat release data in order to understand its effect on the cracking of the material. The results, shown in Fig. 12, indicate that both cement and slag concretes tend to crack when they reach a similar DoR, which emerges as a significant factor in the crack formation process. Consequently, slowing the reaction process may be an effective strategy for delaying crack formation in cementitious materials.

Li et al. [24] investigated the effect of partially substituting slag with metakaolin on the cracking potential using the ring test. The base composition is the same AASF of the previous study, while the modified one (AASFMK) replaced 10% of the slag with metakaolin, which is known to mitigate the autogenous shrinkage [25, 26]. In this case, both compositions were tested at the paste scale using the ring test

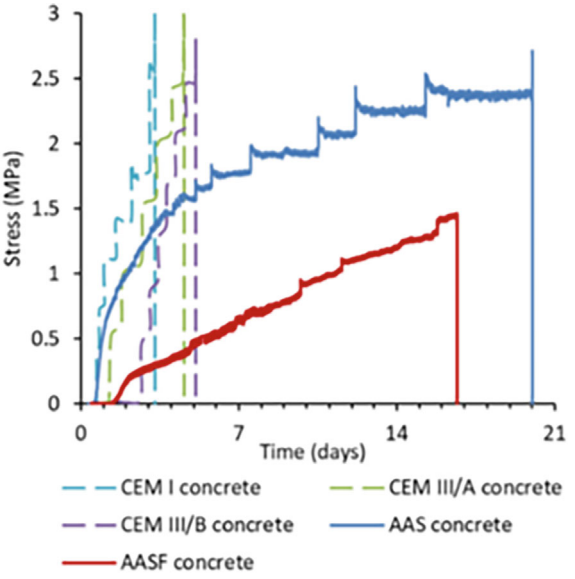


Fig. 9 Autogenous shrinkage-induced stress in alkali-activated concrete (solid lines) and PC concrete (dashed lines) [23]

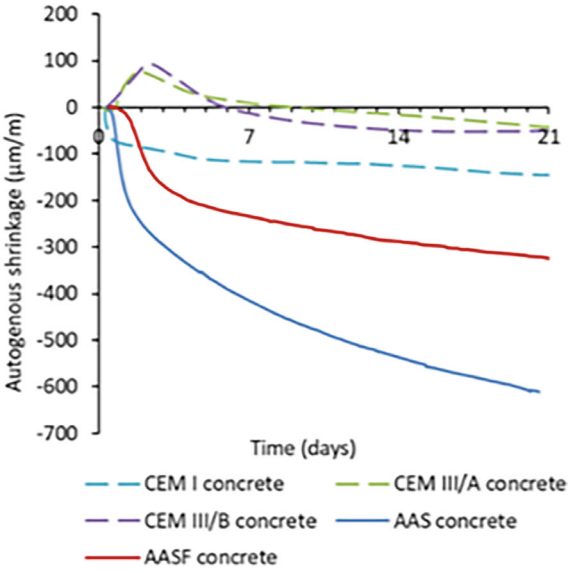


Fig. 10 Autogenous shrinkage of alkali-activated concrete (solid lines) and PC concrete (dashed lines) [23]

with dimensions smaller than described in [9] for concrete. Figure 13 illustrates the positive effect of metakaolin on the cracking potential of the paste: the cracking age is delayed and the maximum stress experienced by the material is increased. In the same study, super absorbent polymers (SAP) were also added to provide internal curing to the material to further reduce the shrinkage (AASFIC and AASFICMK).

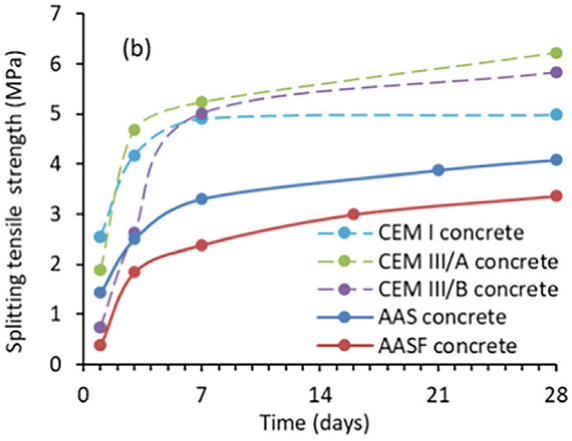


Fig. 11 Splitting strength of alkali-activated concrete (solid lines) and PC concrete (dashed lines) [23]

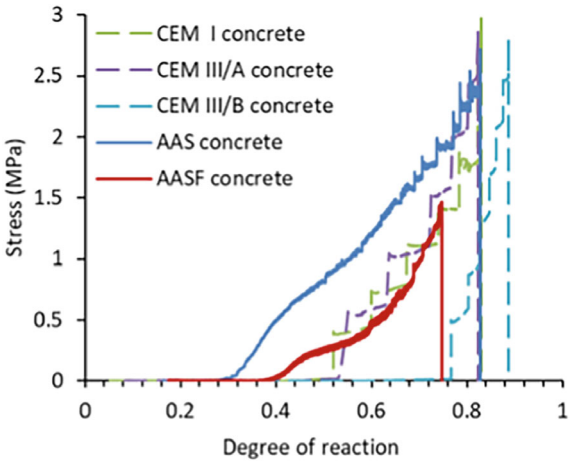


Fig. 12 Autogenous shrinkage-induced stress in alkali-activated concrete (solid lines) and PC concrete (dashed lines) with degree of reaction [23]

In both cases, the addition of SAPs was found to be highly effective in reducing the cracking potential of the material. Notably, AASFICMK did not experience any cracking within the first 100 days. The results are also confirmed by the free autogenous shrinkage performed in parallel, shown in Fig. 14: which demonstrated both metakaolin and SAPs reduce the shrinkage, consequently lowering the stress experienced by the material.

The authors also decided to upscale the most promising composition, AASFICMK, to the concrete scale and compare it to AASF at the concrete scale as well. In this case, the restrained shrinkage test was carried out using the TSTM device. Figure 15 shows that the composition containing metakaolin and SAPs did not experience any cracking within the first 56 days of test, which is consistent with observations made at the paste scale. This further underscores the benefits

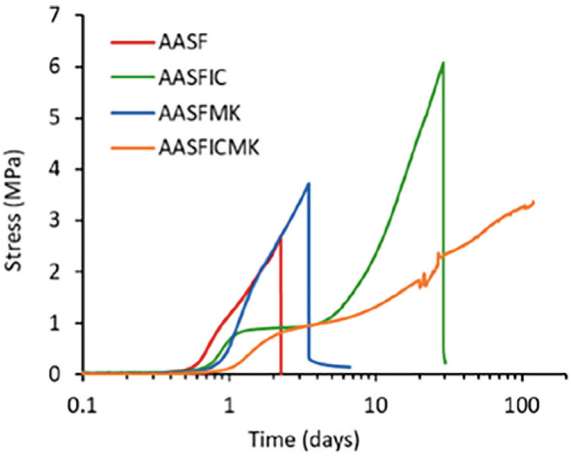


Fig. 13 Autogenous-shrinkage-induced stresses in AASF paste with SAPs (IC for internal curing) and/or MK (metakaolin). The small fluctuation of the stress in AASFICMK paste on around 20 and 30 days was due to the temperature fluctuation in the curing room [24]

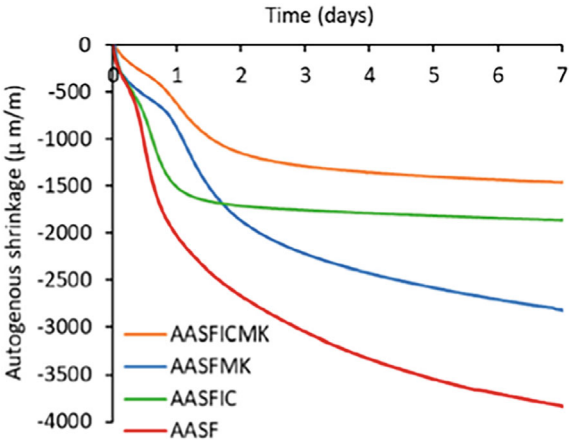


Fig. 14 Autogenous shrinkage of AASF paste with SAPs (IC for internal curing) and/or MK (metakaolin) [24]

of combining metakaolin with superabsorbent polymers to effectively reduce the potential for cracking.

3.2 Restrained Shrinkage in Drying Conditions

Restrained shrinkage under drying conditions attempts to represent better the behaviour of thin elements in which drying is of major importance. One of the few studies on this topic was conducted by Blomart [17]. In that work, the author used the ring test to investigate the same slag composition S05M8 of the previous section [15] but in drying conditions. Specifically, the samples were sealed cured at 20 °C for different periods of time before being exposed to 50 ± 5% relative humidity. To

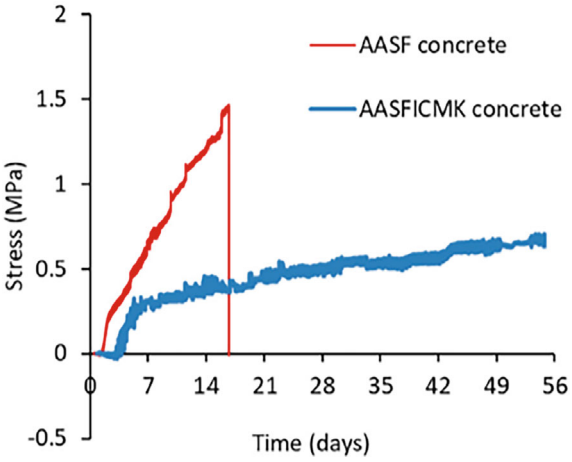


Fig. 15 Self-induced stress in AASF and AASFICMK concrete with SAPs (IC for internal curing) and MK (metakaolin) [24]

ensure that drying occurred solely in the radial direction, the tops of the samples were covered with a double layer of aluminum foil. The curing times of 8, 11, and 24 h were used in order to check the effect of the DoR on the cracking sensitivity. According to the calorimetry tests performed, the DoR increased from 15 to 19% and then to 27% at ages of 8, 11, and 24 h, respectively. The results are summarised in Fig. 16 which also includes data from sealed conditions for better comparison. Even though the cracking time show low repeatability, the maximum strain before cracking is similar for the two samples tested. All the samples exposed to drying present comparable maximum strains, which are lower than those observed under sealed conditions. Notably, the sample cured for 24 h displayed a similar evolution to the sealed samples but cracked shortly after unmoulding, much earlier than the other samples. The author attributes this early cracking to a higher brittleness of the sample, which makes it more susceptible to the humidity gradient developing within the material. In addition, it is also possible that the longer curing period leads to a denser microstructure and reduced permeability, resulting in a stronger humidity gradient and consequently higher stress.

Another study carried out by Ling et al. in 2019 [18] used the ring test at the paste scale, combining fly ash with different sodium silicate-sodium hydroxide solutions. The authors investigated the effect of increasing the solution concentration from 20 to 25% by mass and adjusting the molar ratio between SiO_2 and Na_2O (M_s modulus) from 1.0 to 1.5. Moreover, the authors substituted 2% by weight of fly ash with hexylene glycol as a shrinkage reducing admixture (SRA). In addition, they also tested a type I/II Portland cement composition to use as a reference, both with and without the hexylene glycol. In all cases the s/b ratio was kept constant at 0.33. The samples were seal cured for 24 h at 23 ± 2 °C and then exposed to a 50% relative humidity environment, after sealing the top with paraffin wax to allow only a radial drying of the material. As shown in Fig. 17, increasing the M_s modulus reduces the maximum strain at cracking while delaying the cracking age. On the other hand,

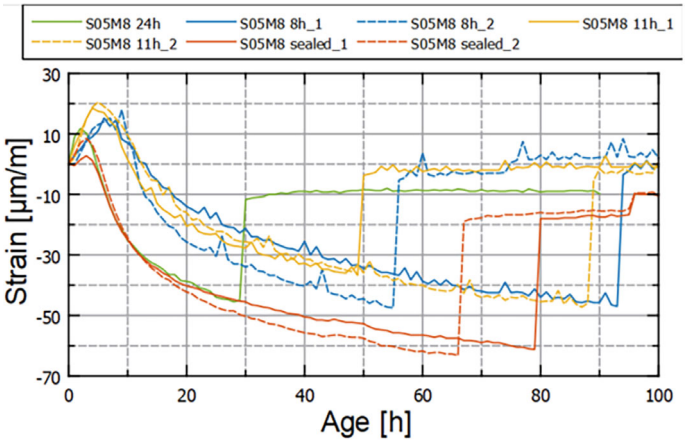


Fig. 16 Ring test comparison in drying conditions for S05M8 (corresponding to a s/b of 0.5 and a molarity of the activator of 8 mol/L) after 8, 11, and 24 h and in sealed conditions based on [17]

higher solution concentrations result in greater maximum strains and earlier failure. These findings are supported by the free deformation results in Fig. 18, which indicate that increasing the M_s modulus reduces shrinkage, while higher solution concentrations increase it. For the free shrinkage results, though, the samples were heat cured at 50 ± 2 °C for seven days before exposed to drying. Finally, the mechanical properties shown in Fig. 19. Compressive strength of PC and fly ash geopolymer pastes with M_s modulus from 1 to 1.5, solution concentration from 20 to 25%, with or without shrinkage reducing admixture SRA [18]. Figure 19, compressive strengths of PC and fly ash geopolymer pastes [18] reveal that an increase in the M_s modulus correlates with reduced strength, while higher solution concentrations enhance strength, allowing the material to accommodate greater deformations without cracking. It is important to point out that, alongside with a reduction in strength, a reduction in the E modulus is also expected when increasing the M_s modulus. The SRA has a beneficial effect as it reduces the maximum strain and delays the cracking time of the samples, while also reducing the free shrinkage of all compositions. From the point of view of PC, its maximum strain in Fig. 17 is comparable to the lowest one obtained for alkali-activated materials. On the other hand, the cracking time is the lowest one of all compositions, both with and without SRA. Similar to findings by Li et al. [23], the strain evolution of OPC is faster than that of alkali-activated mixtures, leading to earlier failure. In contrast, the free deformation results in Fig. 17 display an intermediate behavior between the 20 and 25% concentration compositions. The compressive strength results in Fig. 19 indicate that OPC has the lowest strength at 3 and 7 days but increases at a faster rate than alkali-activated materials up to 28 days.

Another study carried out by Ling et al. in 2019 [18] used the ring test at the paste scale, combining fly ash with different sodium silicate-sodium hydroxide solutions. The authors investigated the effect of increasing the solution concentration from 20 to 25% by mass and adjusting the molar ratio between SiO_2 and Na_2O (M_s

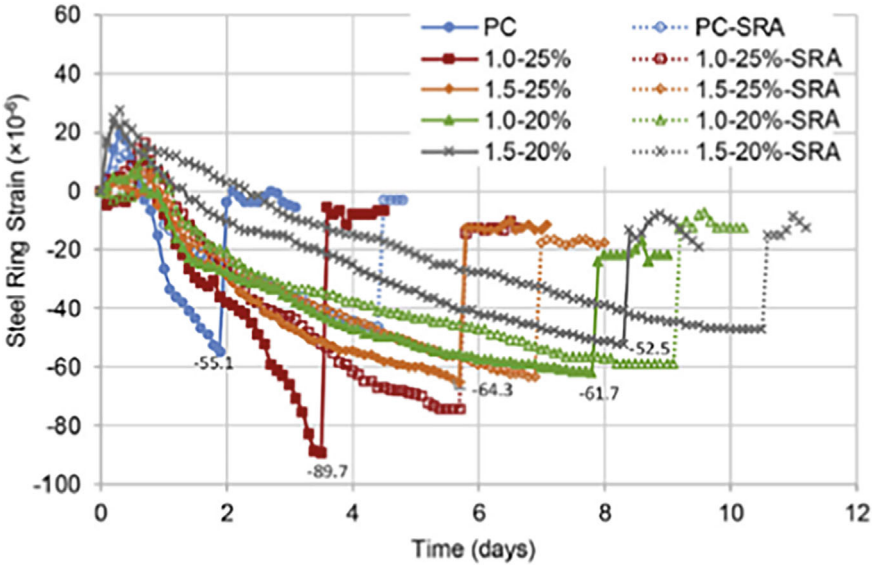


Fig. 17 Restrained ring shrinkage of PC and fly ash geopolymer pastes with M_s modulus from 1 to 1.5, solution concentration from 20 to 25%, with or without shrinkage reducing admixture SRA [18]

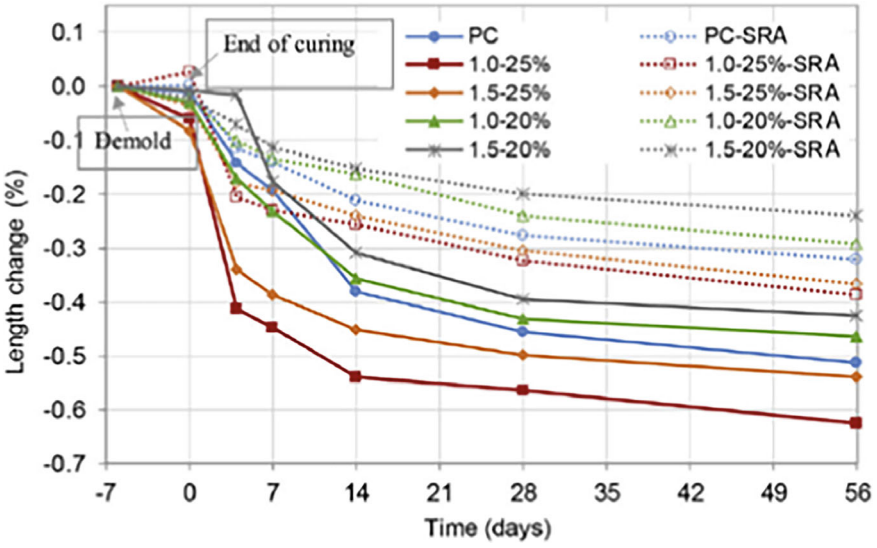


Fig. 18 Free drying shrinkage of PC and fly ash geopolymer pastes with M_s modulus from 1 to 1.5, solution concentration from 20 to 25%, with or without shrinkage reducing admixture SRA [18]

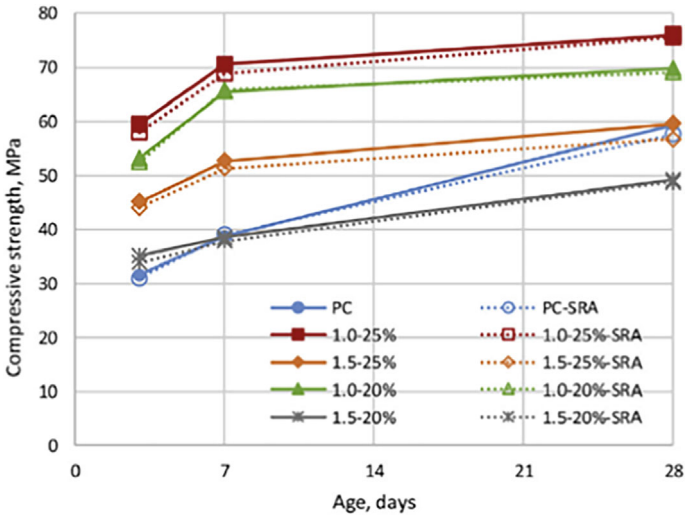


Fig. 19 Compressive strength of PC and fly ash geopolymer pastes with M_s modulus from 1 to 1.5, solution concentration from 20 to 25%, with or without shrinkage reducing admixture SRA [18]

modulus) from 1.0 to 1.5. Moreover, the authors substituted 2% by weight of fly ash with hexylene glycol as a shrinkage reducing admixture (SRA). In addition, they also tested a type I/II Portland cement composition to use as a reference, both with and without the hexylene glycol. In all cases the s/b ratio was kept constant at 0.33. The samples were seal cured for 24 h at 23 ± 2 °C and then exposed to a 50% relative humidity environment, after sealing the top with paraffin wax to allow only a radial drying of the material. As shown in Fig. 17, increasing the M_s modulus reduces the maximum strain at cracking while delaying the cracking age. On the other hand, higher solution concentrations result in greater maximum strains and earlier failure. These findings are supported by the free deformation results in Fig. 18, which indicate that increasing the M_s modulus reduces shrinkage, while higher solution concentrations increase it. For the free shrinkage results, though, the samples were heat cured at 50 ± 2 °C for seven days before exposed to drying. Finally, the mechanical properties shown in Fig. 19. Compressive strength of PC and fly ash geopolymer pastes [18]. Figure 19, compressive strengths of PC and fly ash geopolymer pastes [18] reveal that an increase in the M_s modulus correlates with reduced strength, while higher solution concentrations enhance strength, allowing the material to accommodate greater deformations without cracking. It is important to point out that, alongside with a reduction in strength, a reduction in the E modulus is also expected when increasing the M_s modulus. The SRA has a beneficial effect as it reduces the maximum strain and delays the cracking time of the samples, while also reducing the free shrinkage of all compositions. From the point of view of PC, its maximum strain in Fig. 17 is comparable to the lowest one obtained for alkali-activated materials. On the other hand, the cracking time is the lowest one

Table 2 Mixing proportion of the precursors (% by weight)

Composition	MK (%)	Slag (%)	FA (%)
MKSP 1	80	10	10
MKSP 2	70	20	10
MKSP 3	60	20	20
MKSP 5	50	40	10
MKSP 7	40	50	10
MKSP 4	50	30	20
MKSP 6	40	40	20

Adapted from [19]

of all compositions, both with and without SRA. Similar to findings by Li et al. [23], the strain evolution of OPC is faster than that of alkali-activated mixtures, leading to earlier failure. In contrast, the free deformation results in Fig. 17 display an intermediate behavior between the 20 and 25% concentration compositions. The compressive strength results in Fig. 19 indicate that OPC has the lowest strength at 3 and 7 days but increases at a faster rate than alkali-activated materials up to 28 days.

In another study, Aboshia et al. [19] investigated alkali-activated mortars with seven compositions obtained from the combination of metakaolin with different percentages of slag and fly ash, as detailed in Table 2 All compositions were activated using a mixture of sodium silicate and sodium hydroxide always with the same proportions but with two different s/b ratios of 0.4 and 0.5. In this case, the study was carried out at the mortar scale using a ring test.

From the results in Fig. 20 it is possible to define three groups: the first group includes compositions 1, 2, and 3 where MK is the main precursor; the second group consists of compositions 5 and 7 which have a low percentage of FA; and the third group is composed of compositions 4 and 6 containing 20% of FA. Within each group, reducing the metakaolin content leads to a delay in cracking time and a slight increase in maximum strain at failure. On the other hand, reducing the MK content to 40–50% significantly alters performance based on the FA content: the second group, with only 10% FA, exhibits the poorest cracking potential, while the third group, with 20% FA, demonstrates the best material properties. Increasing the s/b ratio to 0.5 slightly delays the cracking time and reduces the maximum strain without changing the overall behaviour of the different compositions. However, the study does not clarify the influence of free drying shrinkage and mechanical properties on the restrained performance of the materials, as free shrinkage results are only reported under autogenous conditions and mechanical properties are derived from sealed and oven-cured samples. In this case, PC presents the highest maximum strain before failure, comparable to compositions 4 and 6, but has a much shorter cracking time, which is intermediate between groups 1 and 2. The shrinkage evolution of PC appears to be similar to that of the other compositions investigated, unlike the distinctions observed in previous studies.

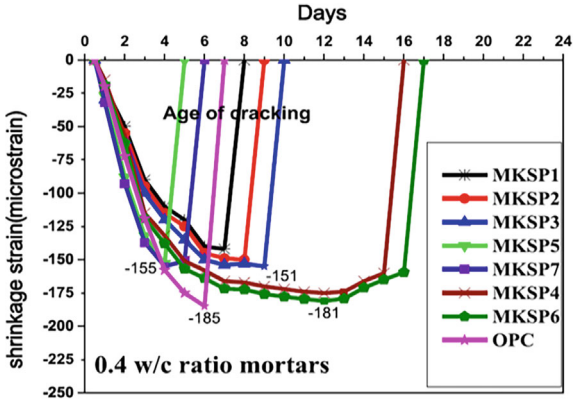


Fig. 20 Average restrained shrinkage strain of MKSP with mixing proportion presented in Table 2 and PC for 0.4 w/c mortars [19]

4 Concluding Remarks

From the studies presented here, it is clear that there is a lack of comprehensive understanding of how alkali-activated materials behave under restrained conditions. However, some key conclusions can be drawn:

1. In sealed conditions, adding fly ash to the slag has a detrimental effect both for the maximum strain and the cracking time, while metakaolin and shrinkage reducing admixtures have a beneficial effect.
2. Changing the activator concentration has different effects depending on the amount of the activator added in the mix.
3. Compared to OPC, alkali-activated systems show higher cracking times due to the lower degree of reaction.
4. Under drying conditions, longer curing periods seem to negatively impact the cracking age of alkali-activated slag.
5. Increasing the concentration of the activating solution increases the free shrinkage and the maximum strain, while reducing the cracking time. On the other hand, increasing the silica modulus has the opposite effect.
6. When metakaolin is the main precursor, increasing the slag content and the fly ash content enhances the cracking sensitivity.
7. Compared to OPC, binary systems present longer cracking times, while in ternary systems cracking time varies with the amount of fly ash.

These findings provide some important insights, although a comprehensive understanding of complex shrinkage and cracking behavior of AAM under restrained conditions is still needed.

References

1. Delsaute, B., Staquet, S.: Testing concrete since setting time under free and restrained conditions. In: Serdar, M., Gabrijel, I., Schlicke, D., Staquet, S., Azenha, M. (eds.) Advanced Techniques for Testing of Cement-Based Materials, pp. 177–209. Springer International Publishing, Cham (2020). https://doi.org/10.1007/978-3-030-39738-8_6
2. Lu, T., Li, Z., van Breugel, K.: Modelling of autogenous shrinkage of hardening cement paste. Constr. Build. Mater. **264**, 120708 (2020)
3. Chen, W., Li, B., Wang, J., Thom, N.: Effects of alkali dosage and silicate modulus on autogenio9xous shrinkage of alkali-activated slag cement paste. Cem. Concr. Res. **141**, 106322 (2021)
4. Ballekere, K.D., Peethamparan, S., Ngami, M.: Autogenous shrinkage of alkali activated slag mortars: basic mechanisms and mitigation methods. Cem. Concr. Res. **109**, 1–9 (2018)
5. Uppalapati, S.: Early-age structural development and autogenous shrinkage of alkali-activated slag/fly ash cements. Ph.D. thesis, KU Leuven, Leuven, Belgium (2020)
6. Collins, F., Sanjayan, J.G.: Effect of pore size distribution on drying shrinking of alkali-activated slag concrete. Cem. Concr. Res. **30**(9), 1401–1406 (2000). https://doi.org/10.1016/S0008-8846(00)00327-6
7. Hossain, A.B., Weiss, J.: Assessing residual stress development and stress relaxation in restrained concrete ring specimens. Cem. Concr. Compos. **26**(5), 531–540 (2004). https://doi.org/10.1016/S0958-9465(03)00069-6
8. Weiss, W.J., Yang, W., Shah, S.P.: Influence of specimen size/geometry on shrinkage cracking of rings. J. Eng. Mech. **126**(1), 93–101 (2000). https://doi.org/10.1061/(ASCE)0733-9399(2000)126:1(93)
9. ASTM C1581/C1581M-18a.: Standard test method for determining age at cracking and induced tensile stress characteristics of mortar and concrete under restrained shrinkage. ASTM International (2024). https://doi.org/10.1520/C1581-04
10. Bentur, A., Kovler, K.: Evaluation of early age cracking characteristics in cementitious systems. Mater. Struct. **36**, 183–190 (2003)
11. Kovler, K.: Testing system for determining the mechanical behaviour of early age concrete under restrained and free uniaxial shrinkage. Mater. Struct. **27**, 324–330 (1994)
12. Delsaute, B.: New approach for Monitoring and Modelling of the Creep and Shrinkage behaviour of Cement Pastes, Mortars and Concretes since Setting Time, Ph.D. thesis. Université Libre de Bruxelles (ULB) (2016)
13. Li, Z., Liang, X., Liu, C., Liang, M., van Breugel, K., Ye, G.: Thermal deformation and stress of alkali-activated slag concrete under semi-adiabatic condition: experiments and simulations. Cem. Concr. Res. **159**, 106887 (2022)
14. Darquennes, A.: Shrinkage of slag cement concrete in free and restrained conditions. In: International RILEM Conference on Volume Changes of Hardening Concrete: testing and Mitigation, Lyngby, Denmark, pp. 165–174 (2006). https://doi.org/10.1617/2351580052.018
15. Sirotti, M., Blomart, S., Delsaute, B., Staquet, S.: Evaluation of the cracking risk in alkali activated materials by means of restrained shrinkage test. In: International RILEM Conference on Synergising Expertise Towards Sustainability and Robustness of Cement-Based Materials and Concrete Structures, SynerCrete'23, vol. 2, pp. 374–384 (2023). https://doi.org/10.1007/978-3-031-33187-9
16. Li, Z., Zhang, S., Liang, X., Ye, G.: Cracking potential of alkali-activated slag and fly ash concrete subjected to restrained autogenous shrinkage. Cem. Concr. Compos. **114**, 103767 (2020)
17. Blomart, S.: Evaluation of the cracking risk in alkali activated materials by means of restrained shrinkage test. Master thesis, ULB, Brussels, Belgium (2022)
18. Ling, Y., Wang, K., Fu, C.: Shrinkage behavior of fly ash based geopolymer pastes with and without shrinkage reducing admixture. Cem. Concr. Compos. **98**, 74–82 (2019). https://doi.org/10.1016/j.cemconcomp.2019.02.007

19. Aboshia, A.M.A., Rahmat, R.A., Zain, M.F.M., Ismail, A.: Early age shrinkage cracking of restrained metakaolin-slag-palm oil fuel ash binder geopolymer mortars. J. Sustain. Cem.-Based Mater. **7**(5), 271–295 (2018). https://doi.org/10.1080/21650373.2018.1485059
20. Luukkonen, T., Abdollahnejad, Z., Yliniemi, J., et al.: One-part alkali-activated materials: a review. Cem. Concr. Res. **103**, 21–34 (2018)
21. Adesina, A., Kavgick, M.: Advancements in the synthesis and processing of alkali-activated materials: activator and precursors. Mater. Today: Proc. (2023)
22. Lacante, M., Delsaute, B., Staquet, S.: Effect of internal and external factors on the volume changes of slag binder activated by sodium hydroxide at early-age. In: International RILEM Conference on Synergising Expertise Towards Sustainability and Robustness of Cement-Based Materials and Concrete Structures, SynerCrete'23, vol. 2, pp. 350–361 (2023). https://doi.org/10.1007/978-3-031-33187-9
23. Li, Z., Delsaute, B., Lu, T., Kostiuchenko, A., Staquet, S., Ye, G.: A comparative study on the mechanical properties, autogenous shrinkage and cracking proneness of alkali-activated concrete and ordinary Portland cement concrete. Constr. Build. Mater. **292**, 123418 (2021)
24. Li, Z., Yao, X., Chen, Y., Lu, T., Ye, G.: A low-autogenous-shrinkage alkali-activated slag and fly ash concrete. Appl. Sci. **10**(17), 6092 (2020). https://doi.org/10.3390/app10176092
25. Li, Z., Nedeljković, M., Chen, B., Ye, G.: Mitigating the autogenous shrinkage of alkali-activated slag by metakaolin. Cem. Concr. Res. **122**, 30–41 (2019). https://doi.org/10.1016/j.cemconres.2019.04.016
26. Li, Z., Liang, X., Chen, Y., Ye, G.: Effect of metakaolin on the autogenous shrinkage of alkali-activated slag-fly ash paste. Constr. Build. Mater. **278**, 122397 (2021). https://doi.org/10.1016/j.conbuildmat.2021.122397